Towards 3D AFM Using Multiple Vibration Modes

Rubin Eyal[1], Bucher Izhak[1], Davis Solomon[1]

[1]Dynamics Laboratory, Mechanical Engineering, Technion
Haifa 3200003, Israel
bucher@technion.ac.il

Abstract

Atomic force microscopy (AFM) is used for measuring nano-scale topographic features. By exciting a micro-cantilever with a sharp stylus at its tip, at or near resonance, a Frequency Modulated AFM (FM-AFM) device can sense the change of resonance frequency due to the change in tip-surface Van der Waals (VdW) potential. The topography is then retrieved from the relationship between the potential and the distance between stylus and the specimen. To improve the measurement speed and address complex geometries emerging in industrial microchip constructions, several enhancements are introduced. While most FM-AFM devices operate in a single vibrating mode, this article enhances existing sensing methods by extending to multidimensional sensing the resonance frequencies that are modulated by the topology, in several orthogonal vibration modes simultaneously. The latter opens new possibilities, e.g. to measure steep walls and trenches or other complex geometries. An Autoresonance (AR) control scheme for faster excitation, and fast frequency estimation algorithm were used for sensing several modes simultaneously, without the need to wait for steady state settling of the cantilever. The concept was tested on a large-scale experimental system, where VdW forces between tip to surface were replaced by magnetic forces, using a magnetic tip and ferromagnetic samples. Experimental results employ 3D relevant topographies such as inclined surfaces, steep walls and trenches that were reconstructed experimentally with 4 (µm) resolution or better. Downscaling to typical AFM dimensions would theoretically yield sub-nanometer resolution. Numerical and experimental data are shown to demonstrate the advantageous of the new approach.

1 Introduction

Atomic force microscopy (AFM) first presented by Binning et al. [1] is used for measuring nano-scale topography features in the semiconductors industry, and for atomic resolution measurments in physics and biology research. The non-contact configuration of the sensor (NC-AFM) is based on a micro-cantilever with a sharp stylus at its tip, vibrating at or near resonance. The tip interacts with the surface, while the distance dependent Van der Waals (VDW) force between the tip and the surface, acts on the cantilever, altering its resonance frequency. A common technique used today is the frequency modulated AFM (FM-AFM), presented by Albrecht et al. [2]. The latter showed that the measured frequency shift correlate to the surface topology.

The present work enhances the one-dimensional measurement capability of current AFM devices to multidimensional measurement capability by allowing the measuring tip to vibrate at two or more directions simultaneously. Here, each direction of excitation is associates to a distinct mode of vibration, hence has a distinct resonance frequency. By measuring the frequency shift in each mode separately, one can evaluate the tip to surface distance in each measured direction [3]. An Auto-resonance (AR) control scheme combined with modal filtering [4] is used for fast frequency tracking of the different modes, and a fast frequency estimation algorithm [5] is used for evaluating the frequency shift. Using this method for two (or more) spatial modes simultaneously results with a multi-dimensional measurement, that has the ability to measure and reconstruct complex geometries. In addition, Since the AR locks into the natural frequency instantaneously, the measuring process can be expedited. This concept was demonstrated in the lab, by a large-scale sensor, where the VdW forces have been replaced by magnetic ones, and the sensing tip is a passive magnet. The sensing tip interacts with a ferromagnetic specimen having a complex topology.

The paper introduces the multidimensional vibrating sensor, demonstrated on a large-scale experimental system in section 2. Section 3 shows some experimental results that are analysed to assess the sensitivity and resolution of the current system. Finally, Section 4 draws some conclusions.

2 Experimental system layout, actuation and sensing

This chapter explains the multimode actuation and sensing concept on the laboratory large-scale experimental system, and the way to interpret the measured data to reconstruct the topology of the measured specimen.

2.1 Multimode actuation and sensing

The measuring magnetic tip is attached to a rectangular cantilever beam which has two orthogonal modes of vibration with distinct natural frequencies at 447 (Hz) and 549 (Hz). Finite element model of the cantilever showing the two direction of motion is illustrated in Figure 1.

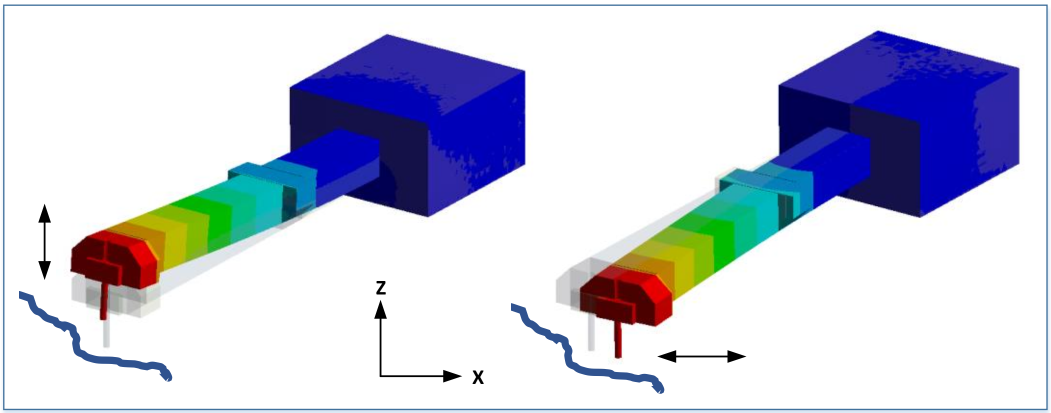

Figure 1: Multidirectional vibration- Left: vetical motion of the tip (z), Right: horizontal motion of the tip (x)

The interaction between the magnetic tip and the surface, due to the magnetic field, contributes to the total potential energy of the cantilever undergoing bending. Hence, one can write:

$$V_{Total} = V_{cantilevel} + V_{ts} = \frac{1}{2}\left(k_x x^2(t) + k_z z^2(t)\right) + V_{ts}(x(t), z(t)) \qquad)1($$

where V_{ts} is the tip to surface interaction potential, k_x, k_z are the modal stiffness and $x(t), z(t)$ are the time dependent modal coordinates of the tip associated with the direction of vibration in x, z respectively.

The magnetic potential depends on the distance between the magnetic tip and the ferromagnetic surface. Hence, the interaction contribution can be added to the constant stiffness matrix of the cantilever:

$$\mathbf{K} = \begin{bmatrix} k_x & 0 \\ 0 & k_z \end{bmatrix} + \begin{bmatrix} \frac{\partial^2 V_{ts}}{\partial x^2} & \frac{\partial^2 V_{ts}}{\partial x \partial z} \\ \frac{\partial^2 V_{ts}}{\partial x \partial z} & \frac{\partial^2 V_{ts}}{\partial z^2} \end{bmatrix} \triangleq \mathbf{K}_0 + \Delta\mathbf{K} \qquad (2)$$

Non-zero of-diagonal terms in $\Delta\mathbf{K}$ indicates that the specimen is inclined. In the present research, the information in x and z appears at 2 distinct frequencies and we obtain only the diagonal terms of $\Delta\mathbf{K}$, one at a time. The distance of the tip to the specimen is deduced from these terms only.

In order to excite each direction at a different frequency simultaneously we employ modal control according to the configuration shown in Figure 2. The cantilever is excited with two voice-coil actuators placed symmetrically at $45°$ on both sides of the cantilever. Two laser displacement sensors (Keyence LK-H008) are also positioned at $45°$ on both sides of the cantilever measuring the displacement of the cantilever close to the tip. Modal filtering [6] is performed digitally in order to project the measured data and excitation forces on the exact modes directions.

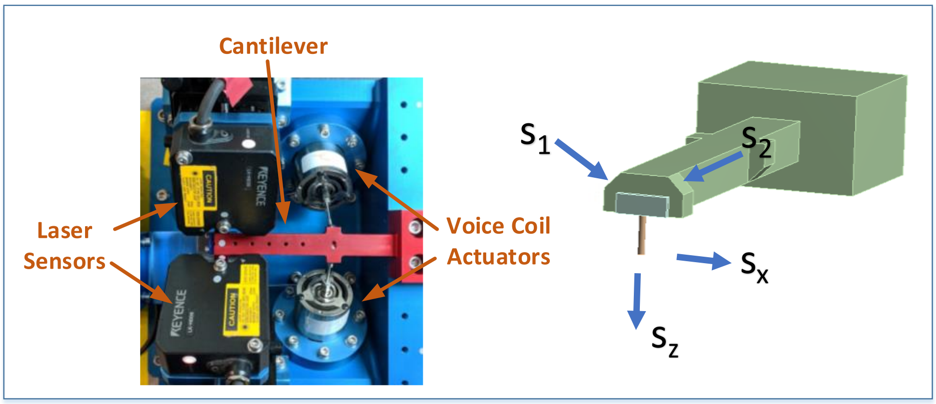

Figure 2: Left: laboratory realization using 2 voice-coil actuators acting at 45 degrees, and two optical (Keyence™) sensors measure in the same directions. Right: Illustration of the measurement of two sensors from inclined surfaces on the cantilever close to the magnetic tip.

The modal filtering (MF) uses the bi-orthogonality between the vibration modes, by taking a linear combination of the two sensors signals so that all modes are canceled but one. An illustration for the modal filtering of the displacement signals, measured by the laser sensors, is presented in

Figure 3 , where S_1, S_2 are real measured signals and S_z, S_x are the modal filtered displacements from the following equation:

$$\begin{aligned} S_x(t) &= S_1(t) - S_2(t) \\ S_z(t) &= S_1(t) + S_2(t) \end{aligned} \tag{3}$$

The separation of modes can be clearly seen on the frequency domain after applying a fast Fourier transform (FFT) to the measured and modal-filtered signals. The latter is demonstrated on the measured signals, and a similar approach is performed on the excitation forces operating on the cantilever by two voice-coil actuators.

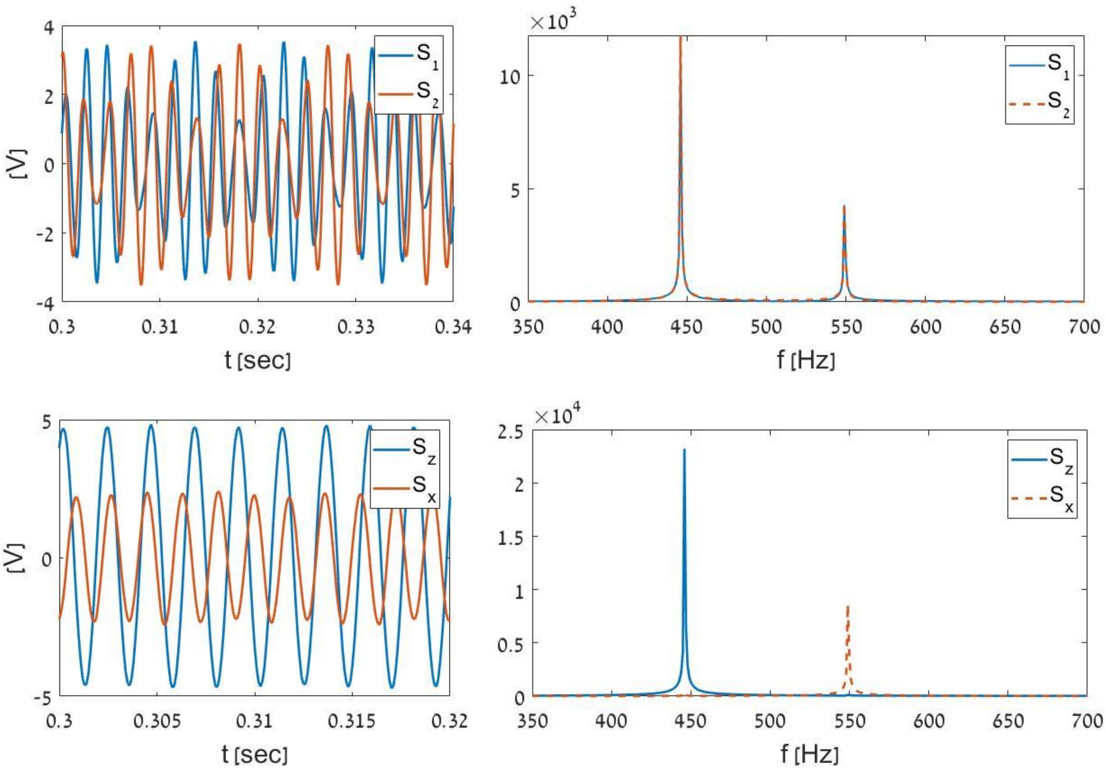

Figure 3: Top-left: measured signals S_1, S_2 from the experimental system. Top-right: S_1, S_2 frequency content showing both resonance frequencies are present in both measured signals. Bottom-left: S_x, S_z after applying modal filtering (3). Bottom-right: S_x, S_z frequency content showing the separation of frequencies in the modal-filtered signals.

Modulation of the natural frequency is detected by auto-resonance (AR) resonance tracking control scheme, combined with a new frequency estimation algorithm [5] , that uses Linear Least Squares (LLS) to fit an instantaneous phase to the noisy signal for several periods, and then fits a time dependent line whose slope is an estimate of the signal's frequency. Autoresonance, also known as self-excitation, is a well-known nonlinear feedback method used for automatically exciting a system at its natural frequency [7], [8]. It locks into resonance from the first cycle, and has the potential to increase the imaging speed compared to the common scheme employed in AFM - Phase Locked Loop (PLL), whose frequency locking speed is greatly reliant on the settling time of the cantilever. Both resonance tracking and frequency estimation are performed simultaneously for the two modes of vibration using modal filtering.

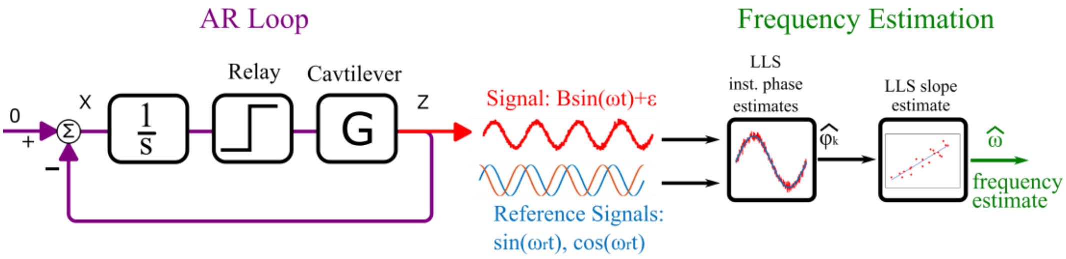

Figure 4: Schematic digram of the resonance tracking and frequency estimation. The AR feedback loop described here consist of a phase shifting element P which shifts the phase of the input signal by 90 degrees, and a digital 'relay' or sign function that forces the amplitude of the input signal to constant values [4].

Assuming white noise, the variance of the frequency estimated using the frequency estimation algorithm [5] depends significantly on the total estimation time t_N, and also on the sampling rate and on the SNR - signal to noise ratio between the variance of the single tone signal without the noise, to the variance of the noise. This variance bounds the minimal frequency shift (Δf_{min}) that can be measured by the sensor. Measurement accuracy and speed should be balanced for a desired working point.

$$\sigma_f^2 \approx \frac{12}{F_s t_N^3 SNR} \tag{4}$$

2.2 From frequency modulation to surface topology identification

Two main scanning methods can be used to scan a specimen [9]: Constant height or constant gap (frequency). In the former the probe is located in a constant height above the surface, and the change is the resonant frequency is measured and then converted into the change in surface topography. In the latter, the gap between the probe and the sample stays constant using a standard PI control scheme that keeps a constant natural frequency for single and dual mode excitation. In the large-scale demonstrator presented in this paper, an XYZ stage instantaneous location (with a $0.2\,\mu m$ resolution) was used for the surface topology estimation.

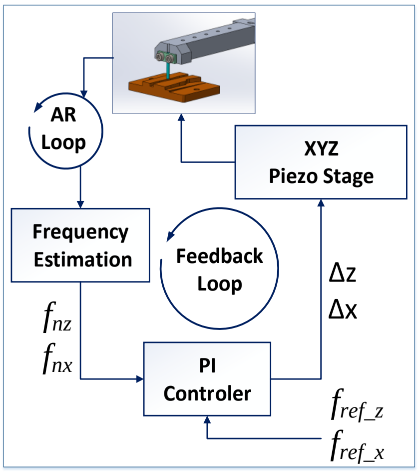

Figure 5: Control scheme for position control. The feedback loop keeps a constant resonance frequency by changing the position of the sample relative to the vibrating tip, keeping a constant gap between them. The XYZ stage displacements are then use to reconstruct the surface topology.

2.3 Laboratory experimental system implementation

The abovementioned measuring methodology is demonstrated using a large-scale experimental system. A schematic layout of the system is presented in Figure 6. The main subsystems consist actuation of the cantilever beam using two voice-coil actuators, measurement of the beam tip displacement using two optical sensors (Keyence™), and specimen displacement using XYZ accurate piezo stage (Nanomotion™). All the vibrating parts are mounted on an optical table through a rigid aluminum base in order to decrease the peripheral vibrations of the system, as detailed in Figure 7. The measured and actuation signals are generated in real time by a Xilinx FPGA connected to a dSpace™ signal processor, and are integrated to Matlab, together with the XYZ stage control.

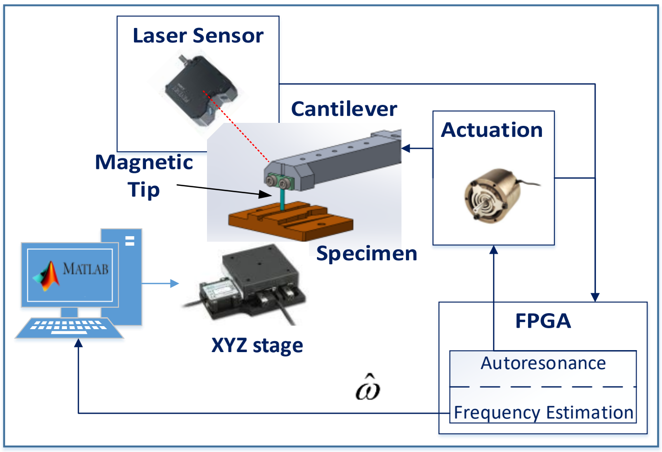

Figure 6: Large-scale experimental system layout

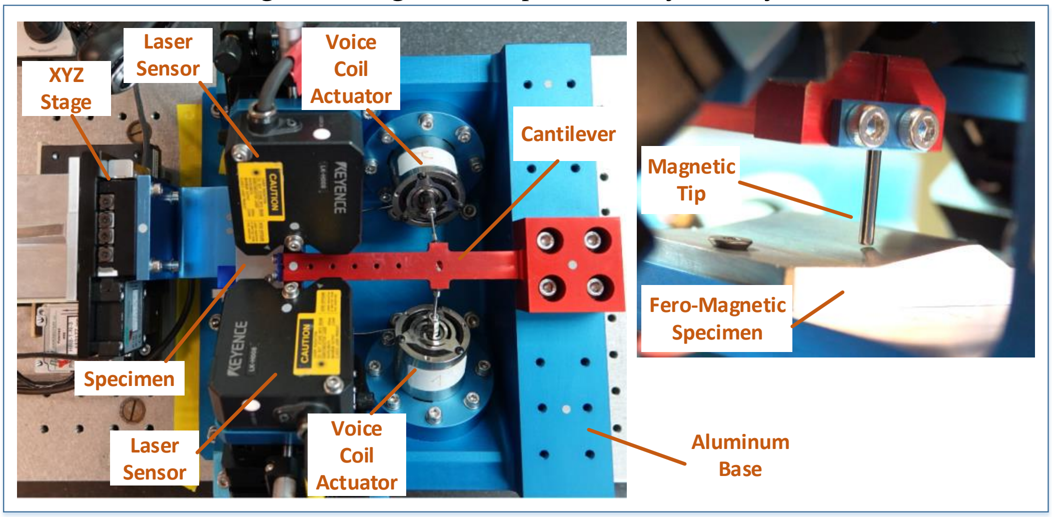

Figure 7: Detailed view of the large scale experimental system. Cantilever beam (in red) length- 130 mm and cross-section- 12mm X 15mm. Magnetic tip diameter- 2 mm and length- 20 mm

3 Experimental results

This chapter will present some of the main measured results of the large-scale experimental system, together with resolution and performance analysis and a relevant down-scale approximation to a real AFM.

3.1 Main results

First result in fig8 show the nonlinear dependency between the tip-surface distance (gap) and resonance frequency that effects the sensitivity of measurement for different gaps. Though, for small gaps and small oscillations (i.e. around 0.1 mm), linear relationship is obtained. Furthermore, once the control system (presented in chapter 2.2) moves the specimen to obtain the same reference frequency, the gap also remains the same, and the nonlinear dependency is effectively eliminated. Hence, the measurement is carried out with the same sensitivity.

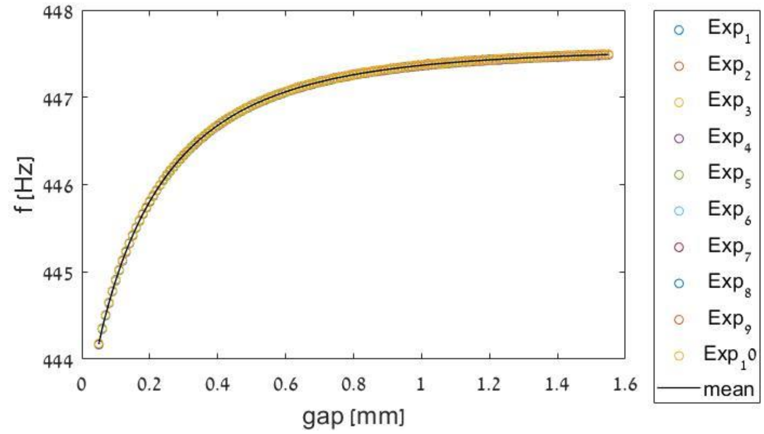

Figure 8: Dependency of resonance frequency on the distance between the measuring tip and the specimen. The experiment was repeated 10 times showing repeatability.

Steep and complex geometries, such as walls, grooves and trenches cannot be fully reconstructed by measuring a single spatial direction. Using the multidimensional measurement method presented in this paper, complex geometries were reconstructed experimentally as demonstrated in Figure 9: Left: measuring tip next to the steep walled and narrow trench specimen. Right: reconstructed geometry showing both the geometry of the wall and of the inclined bottom surface (3D).Figure 9 and Figure 10.

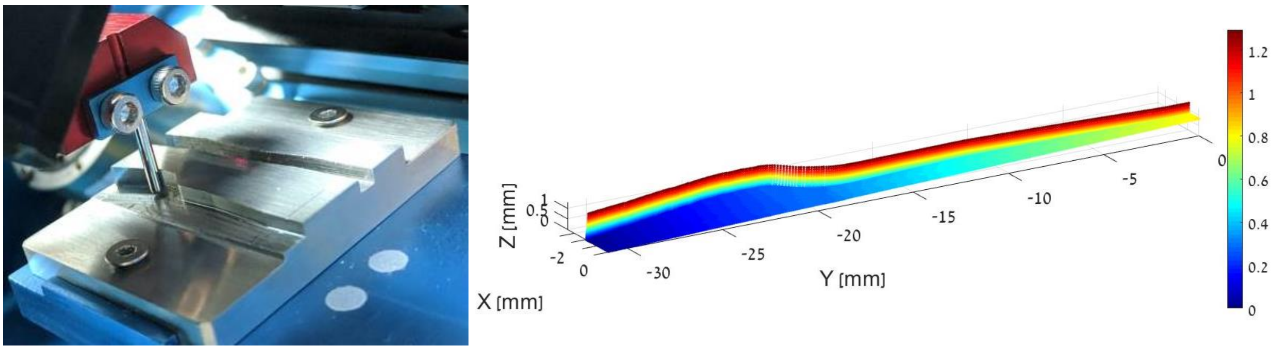

Figure 9: Left: measuring tip next to the steep walled and narrow trench specimen. Right: reconstructed geometry showing both the geometry of the wall and of the inclined bottom surface (3D).

The narrow trench geometry shown on the left in Figure 10 has been reconstructed, including the steep walls curvature and slight machined angle of the bottom surface. Still, since the magnetic field is not as localized as VdW forces in AFM, parasitic cross coupling effects distort the reconstructed geometry. These effects are not expected to occur on the nanoscale where tip-sample interaction, dominated by the local VdW forces, is more localized then the magnetic forces employed here.

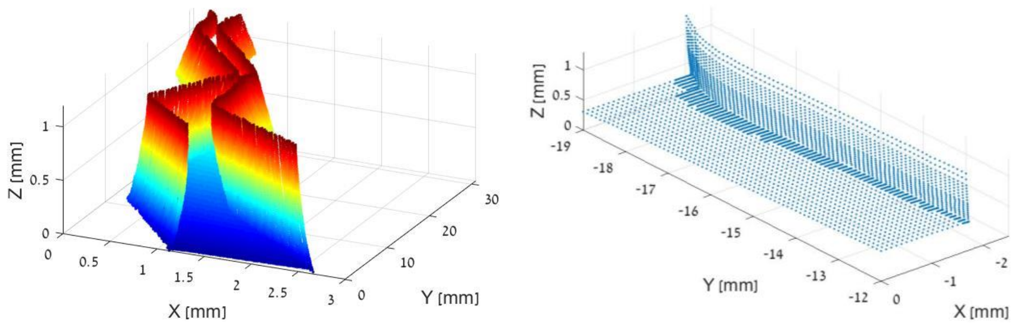

Figure 10: Left: reconstructed geometry of a narrow trench. Right: scanning step size manipulation using multiple mode information. Near the right angled corner, small steps were taken, which was made possible by sensing both vertical and horizontal gaps

The right side of **Error! Reference source not found.** illustrates the use of the additional information in each measuring point for improving the scanning algorithm, e.g. decreasing the scanning step size in advance, while approaching a vertical wall by using the horizontal sensing mode to sense that the geometrical gradient become large.

3.2 Performance analysis

The experimental system is a large scaled AFM, hence the performance should be compared to a commercial FM-AFM [10] using relevant scaling factor. Magnet size, shape and orientation, spatial resolution of XYZ stage, frequency estimation resolution, sensors resolution, external disturbances and noise are some of the many parameters affect the measuring resolution of the large-scale experimental system. The resolution of the commercial AFM was measured for a specific image size, hence a similar method was exploit in the large-scale system. As consequence, a suitable non-dimensional comparison is the ratio between the resolution and the image size. The resolution of the large-scale experimental system was measured by scanning a flat rectangular surface with 10,201 data points, and calculating the standard deviation of the measurements. The RMS measured resolution is 1.3 (μm) for the vertical mode (z), and 4 (μm) for the horizontal mode (x). The reason for the difference between the modes is the spatial effects of the magnetic field created from the cylindrical shape of the magnet. The magnetic forces that affect the frequency shift are larger in the vertical direction, parallel to the axis of the cylindrical magnet, hence the resolution in the vertical direction is better.

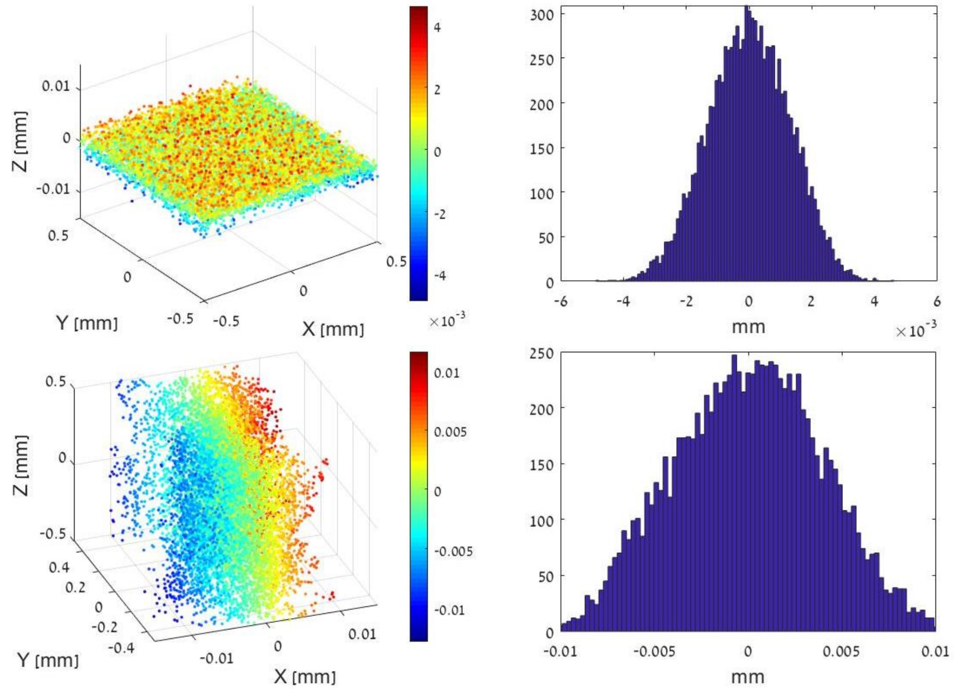

Figure 11: Total resolution measurement of the large-scale experimental system. Top left: vertical mode (z) measured data points. Top right: statistical analysis for the vertical mode showing a histogram representing the measured gap probability distribution. Bottom left: horizontal mode (x) measured data points. Bottom right: statistical analysis for the horizontal mode.

Table 1 compares the large-scale experimental system to a commercial FM-AFM system [10] showing similarity in non-dimensional parameters $\Delta f_{min} / f_0$ and resolution/image size, where f_0 is the basic resonance frequency of the cantilever, and Δf_{min} is the minimal measured frequency shift. The similarity approves the validity of the up-scaling done in the demonstration of the multidimensional measuring method.

Parameter	Commercial AFM [10]	Large Scale System Vertical Mode (z)	Large Scale System Horizontal Mode (x)
f_0 (Hz)	$330 \cdot 10^3$	447	549
Δf_{min} (Hz)	20	0.012	0.012
$\Delta f_{min} / f_0$	$6.06 \cdot 10^{-5}$	$2.68 \cdot 10^{-5}$	$2.18 \cdot 10^{-5}$
image size	0.2 (μm)	1 (mm)	1 (mm)

resolution	0.38 (nm)	1.3 (μm)	4 (μm)
resolution/image Size	0.0019	0.0013	0.004

Table 1: comparing parameters between a commercial AFM to the large-scale experimental system

4 Conclusions

A method able to measure complex geometries with multidirectional probe has been presented. The method combines modal filtering with Autoresonance, for fast resonance tracking, simultaneously in two or more spatial directions. The method was demonstrated on a large-scale experimental system that was able to reconstruct 3D relevant topographies, such as inclined surfaces, steep walls and trenches, with 4 (μm) resolution or better. A nano-scale system based on the same principles is currently being constructed, and is expected to improve measurement speed and ability to measure complex geometries with Angstroms resolution.

Acknowledgments

This research has been funded by The Israel Innovation Authority, within Multi-Dimensional Metrology (MDM) Consortium, 2018-2020.

References

[1] G. Binnig, C. Gerber, and C. F. Quate, “Atomic Force Microscopy,” *Phys. Rev. Lett.*, vol. 56, p. 930, 1986.

[2] T. R. Albrecht, P. Grütter, D. Horne, and D. Rugar, “Frequency modulation detection using high-Q cantilevers for enhanced force microscope sensitivity,” *J. Appl. Phys.*, vol. 69, no. 2, pp. 668–673, 1991.

[3] F. J. Giessibl, “A direct method to calculate tip-sample forces from frequency shifts in frequency-modulation atomic force microscopy,” *Appl. Phys. Lett.*, vol. 78, no. 1, pp. 123–125, 2001.

[4] S. Davis and I. Bucher, “Automatic vibration mode selection and excitation; combining modal filtering with autoresonance,” *Mech. Syst. Signal Process.*, vol. 101, pp. 140–155, 2018.

[5] S. Davis and I. Bucher, “A new approach to single-tone frequency estimation via linear least squares curve fitting,” Apr. 2019.

[6] L. Meirovitch and H. Baruh, “Control of Self-Adj oint Distributed-Parameter Systems,” *J. Guid. Control. Dyn.*, vol. 5, no. 1, pp. 60–66, 1982.

[7] W. E. Vander Velde, “Multiple-input describing functions and nonlinear system design.” McGraw-Hill, New York, 1968.

[8] K. J. ÅStröM, “Oscillations in Systems with Relay Feedback,” pp. 1–25, 2011.

[9] N. C. Santos and F. A. Carvalho, *Atomic Force Microscopy Methods and Protocols*. 2019.

[10] H. Seo, D. Goo, G. Jung, R. Stomp, and J. Wei, “Park NX-Hivac : Phase-lock Loop for Frequency Modulation Non-Contact AFM,” *Park AFM SYSTEMS*. [Online]. Available: https://www.parksystems.com/index.php/applications/manufacturing/semiconductor/197-high-throughput-and-non-destructive-sidewall-roughness-measurement-using-3-dimensional-afm. [Accessed: 04-Apr-2019].